

The giant plasticity of a quantum crystal

Ariel Haziot¹, Xavier Rojas¹, Andrew D. Fefferman¹, John R. Beamish^{1,2}, and Sébastien Balibar¹

1- *Laboratoire de Physique Statistique de l'École Normale Supérieure,
associé au CNRS et aux Universités P.M. Curie and D. Diderot,
24 rue Lhomond, 75231 Paris Cedex 05, France.*

2 - *Department of Physics, University of Alberta, Edmonton, Alberta Canada T6G 2G7*

When submitted to large stresses at high temperature, usual crystals may irreversibly deform. This phenomenon is known as plasticity and it is due to the motion of crystal defects such as dislocations. We have discovered that, in the absence of impurities and in the zero temperature limit, helium 4 crystals present a giant plasticity that is anisotropic and reversible. Direct measurements on oriented single crystals show that their resistance to shear nearly vanishes in one particular direction because dislocations glide freely parallel to the basal planes of the hexagonal structure. This plasticity disappears as soon as traces of helium 3 impurities bind to the dislocations or if their motion is damped by collisions with thermal phonons.

PACS numbers: 67.80.de, 67.80.dj, 62.20.fq, 62.20.de

A crystal resists elastically to a shear stress, contrary to a fluid, which flows. When applied to a crystal, a small shear stress σ produces a strain ε that is proportional to σ . If the stress is released, the crystal returns elastically to its original shape. The elastic shear modulus of the crystal is the ratio $\mu = \sigma/\varepsilon$. However, if the applied stress is large, a usual crystal is "plastic": it deforms more than in the elastic regime thanks to the motion of dislocations. With classical crystals, plastic deformation is irreversible and small. In metals, it requires stresses of order 10^{-1} to 10^{-6} of the shear modulus and the strain rate increases with temperature [1, 2]. We have discovered that, in the case of ultrapure helium 4 single crystals around 0.1 K, the resistance to shear nearly vanishes in one particular direction while in another direction no measurable deviation from normal elastic behavior occurs. This giant anisotropic plasticity is independent of stress down to extremely low values (10^{-11} times the elastic shear modulus). We demonstrate that it is a consequence of dislocations gliding freely along the basal planes of the hexagonal crystal structure. Some gliding along these planes had been observed [3, 4] in other hexagonal crystals but never with comparable amplitude. In ^4He crystals, we show that dislocations are able to move at high speed with negligible dissipation so that the plasticity is also independent of the rate at which the strain is applied. Moreover, this motion is reversible so that the plasticity shows up as a 50 to 80% reduction of one particular elastic coefficient, which we have identified as c_{44} . The plasticity disappears if traces of impurities bind to dislocations or if thermal phonons damp their motion. Our observations have been made possible by direct elasticity measurements on oriented crystals where the impurity concentration could be lowered from 0.3 ppm to zero at very low temperature (15 mK). The gliding of dislocations is an intensively studied phenomenon of fundamental importance in Materials Science [5]. We provide strong experimental evidence for its precise origin.

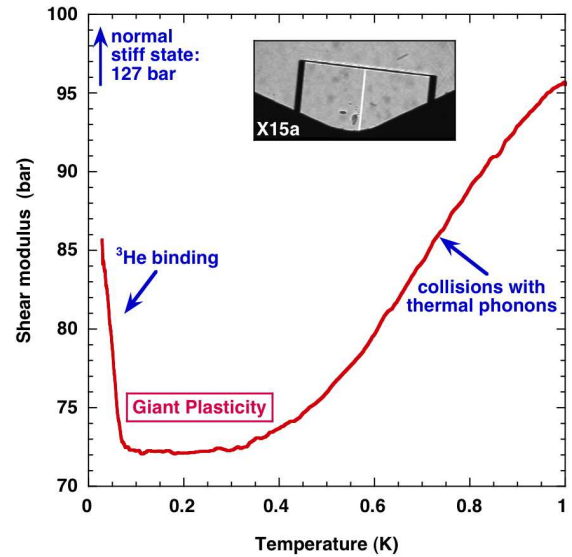


FIG. 1: The shear modulus of crystal X15a as a function of temperature. Around 0.2 K, the shear modulus is reduced to 72 bar, much less than the normal value (127 bar).

We have improved some of our previous techniques [6–9]. Here we briefly describe them (see details in the Supplemental Material). In a transparent cell inside a dilution refrigerator with optical access, crystals can be seen during growth. After determining their orientation from their shape (Fig. 1), we grow them in a 1 mm gap between two piezo-electric transducers. Applying a small ac-voltage to one transducer (0.001 to 1 Volt, 200 to 20,000 Hz) produces a vertical displacement (0.001 to 1 Angstrom) and consequently a strain ε of amplitude 10^{-10} to 10^{-7} and a stress $\sigma = \mu\varepsilon$ (10^{-9} to 10^{-5} bar) on the other transducer (μ is the relevant shear modulus of the crystal). The stress generates a current that is our signal after amplification with a lock-in. The shear modulus μ and the dissipation $1/Q$ are obtained from

the magnitude and phase of the signal. Various growth methods lead to three different types of crystals [7]:

1 - High quality "type 1" crystals are grown by pressurizing the superfluid liquid in the cell at 20 mK up to the crystallization pressure and staying there after the cell is nearly full. Random nucleation produces different orientations. In this case, there remains some liquid in corners but not in the gap. Fresh from growth, such crystals are totally free of impurities, especially if one uses ultrapure ^4He containing 0.4 ppb of ^3He (we also use natural ^4He with 0.3 ppm ^3He). Slow growth at 20 mK rejects ^3He impurities in front of the liquid-solid interface as in the "zone melting" purification of metals but here this method is extremely efficient because the temperature is very low [8]. However, when warming such ultrapure crystals, ^3He impurities come back into the crystal where their concentration varies with temperature.

2 - Single crystals of lower quality (type 2) are grown at 1.4 K. All the remaining liquid is crystallized during further cooling along the melting line from 26.1 bar at 1.4 K to 25.3 bar at 1 K, below which it stays constant [10]. This pressure change probably creates dislocations, but the ^3He concentration is that of the helium gas used to grow them. Any type 1 crystal can be melted down to a small seed and regrown at 1.4 K as a type 2 crystal with the same orientation, or vice versa.

3 - Polycrystals (type 3) are grown at constant volume starting with normal liquid at 3 K and 60 bar.

Fig. 1 presents a measurement of the shear modulus μ of crystal X15a at 9 kHz during cooling. This is an ultrapure type 1 crystal, although grown at 600 mK. Its shear modulus reaches a very small value around 0.2 K. At lower T , the crystal stiffens as a consequence of dislocation pinning by ^3He [6, 9, 11]. Crystals with immobile dislocations are stiffer than with mobile dislocations. The pinning temperature depends on the ^3He concentration, on the binding energy $E_3 = 0.73$ K [11], and on the measurement frequency. Above 0.3 K, μ also increases, probably because dislocations scatter thermal phonons [12]. We thus understand that ^4He crystals show an anomalous shear modulus between impurity pinning at very low T and collisions with thermal phonons at higher T . We call it a "giant plasticity" because it is due to the large motion of dislocations under very small stresses. Since it is reversible, the plasticity shows up as a reduction in the shear modulus. Note that the present measurements are made at kHz frequencies during hours with results that are independent of the sign and duration of the applied strain.

Two type 2 crystals are compared in Fig. 2a: X15c (purity 0.4 ppb) and X21 (0.3 ppm ^3He), at high or low driving strain. When a larger drive is applied, the temperature at which ^3He bind to dislocations is lower, so that the plasticity domain is wider. As expected [6, 9, 11], pinning by ^3He occurs at lower T for ultrapure crystals. Fig. 2b shows the corresponding dissipation. In the plas-

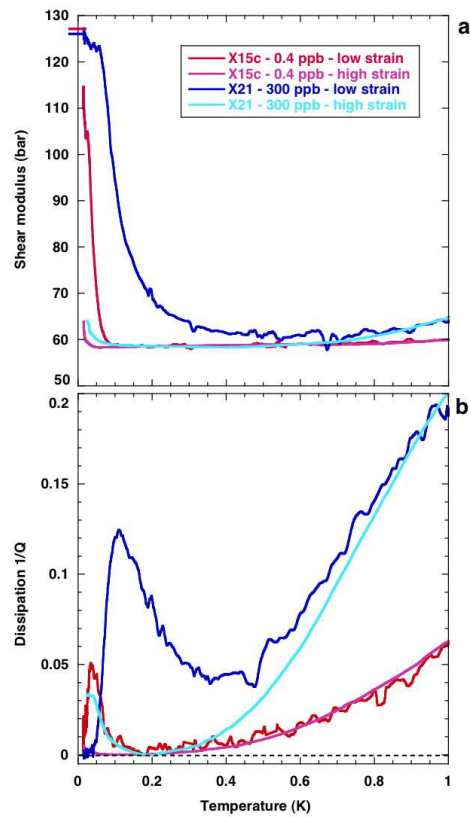


FIG. 2: Comparison of two "type 2" crystals: X15c and X21 grown respectively from ultrapure and from natural ^4He . The T -domain of the giant plasticity depends on both purity and strain amplitude. On graph (a), two ticks on the vertical axis indicate the predicted value of the shear modulus for immobile dislocations. The lower graph (b) shows that the dissipation is negligible in the high plasticity region of X15c, as for immobile dislocations in the zero temperature limit of X21.

ticity domain of X15c, we measure zero dissipation, as in the low T limit of X21 where ^3He binding suppresses dislocation motion. The peak dissipation corresponding to ^3He binding is lower in temperature for the ultrapure crystal X15c and it nearly disappears at a high strain $\varepsilon = 10^{-7}$ that exceeds the threshold for ^3He unbinding ($3 \cdot 10^{-8}$, see [6, 13]). The dissipation above 0.3 K is independent of amplitude and increases with T as expected for a thermal phonon scattering mechanism [12].

We have identified the precise origin of the plasticity with the following quantitative study. Hexagonal crystals have 5 independent elastic coefficients [13–15] c_{11} , c_{12} , c_{13} , c_{33} , c_{44} and $c_{66} = (c_{11} - c_{12})/2$. The indices 1 to 6 respectively refer to xx , yy , zz , yz , xz and xy , where z is the $[0001]$ "c" axis. Fig. 3 shows results from 7 type 2 crystals, all of natural purity except the ultrapure X15, and one polycrystal (BC2). X3 is tilted with a c -axis 45° from the vertical. Its effective shear modulus is $\mu = 0.004 c_{44} + 0.004 c_{66} + 0.25 (c_{11} + c_{33} - 2c_{13})$, practically independent of c_{44} and c_{66} (see Suppl. Mat.). It shows

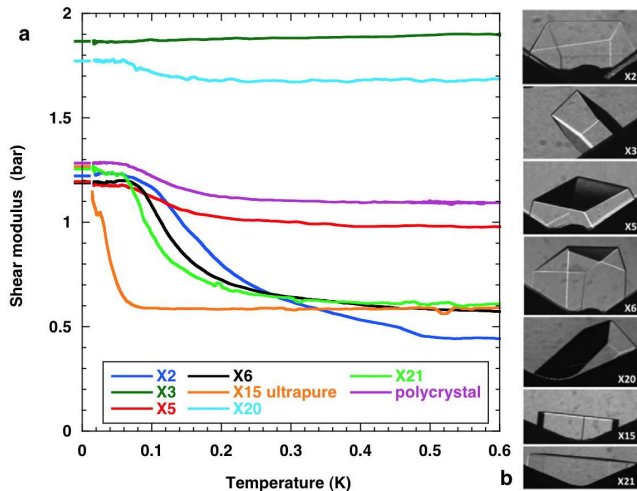


FIG. 3: Measurements (a) for different crystal orientations show that the plasticity is highly anisotropic. Ticks on the vertical axis show the predicted shear modulus with immobile dislocations, in excellent agreement with measurements in the low temperature limit where dislocations are pinned by ^3He .

no T -dependence. Since it is very unlikely that these coefficients would vary with T in just such a way to keep $(c_{11} + c_{33} - 2c_{13})$ constant, we conclude that c_{12} , c_{13} and c_{33} are independent of T , so that X3 could be used to calibrate the piezo-electric coefficient of our transducers (0.88 Angstrom/Volt in our first cell, 0.95 in the second cell). For this we used values of elastic coefficients measured from ultrasound velocity at the melting pressure [14, 15] $c_{11} = 405$ bar, $c_{12} = 213$ bar, $c_{13} = 105$ bar, $c_{33} = 554$ bar, $c_{44} = 124$ bar, and $c_{66} = 96$ bar. These values correspond to the intrinsic elasticity of ^4He crystals because dislocations could not move at 10 MHz above 1.2 K. Given this calibration we could calculate the shear modulus for all other orientations in the $T=0$ limit (ticks on the vertical axis of Fig. 3). Excellent agreement is found with our measurements except for X15 whose stiffening was not completed at 15 mK. For the polycrystal BC2, Maris' averaging method [16] leads to excellent agreement again.

All crystals except X3 show a strong T -dependence, which could be due to a reduction of either c_{44} or c_{66} . Indeed, hexagonal crystals usually have one preferential gliding plane that can be either the basal plane (0001) or the prismatic planes perpendicular to it. For hcp crystals, it is predicted to be the basal plane, although directional bonding in hexagonal metals can lead to non-close packed structures which favour prismatic glide [3, 4]. For X21, the dependence on c_{66} is negligible and the large variation of c_{44} could be easily extracted. Assuming then that c_{66} is constant, we could calculate the variation of c_{44} in all crystals. Since X2, X5, X6 and X21 were all type 2 crystals grown in similar conditions, one expects the T -

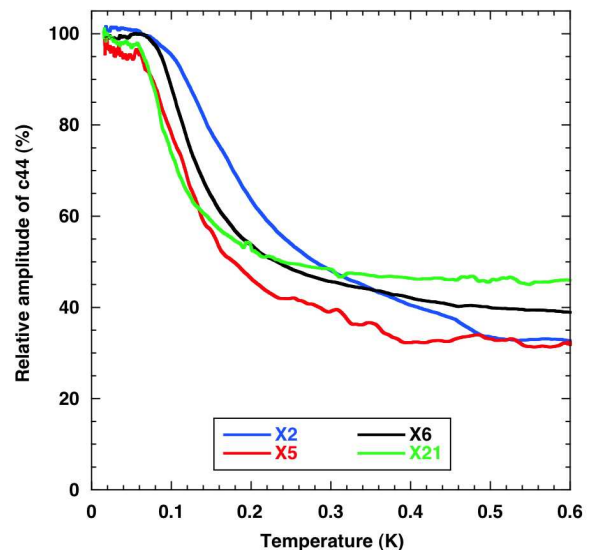


FIG. 4: Assuming that dislocations glide in the basal plane, one finds the same variation of c_{44} by 62 ± 8 % for X2, X5, X6 and X21, which are crystals with different orientations grown in the same conditions. Assuming that they glide in the prismatic planes leads to absurd results (see text).

dependence of their coefficient c_{44} to be the same. Fig. 4 shows that this assumption leads to a reproducible reduction of c_{44} (62 ± 8 % for all type 2 crystals), although the shear modulus of X2 depends mostly on c_{44} while that of X5 depends mostly on c_{66} . On the opposite, assuming that c_{44} is constant and c_{66} varies leads to absurd results: from 60% reduction in c_{66} for X5 to 300% for X6 and to 1000 % for X2, not mentioning X21. The preferential direction for gliding has to be the basal plane. Only c_{44} depends on temperature. This is why Fig. 3 shows a highly anisotropic plasticity.

The amplitude dependence is also consistent with ^3He pinning at low T . Fig. 5 shows the shear modulus as a function of stress for 4 crystals at 20 mK. Above a $1 \mu\text{bar}$ threshold due to the breakaway from ^3He impurities [6, 13], the shear modulus decreases. By projecting the stress on the basal plane, we determined the "resolved stress" (see Suppl. Mat.), and we obtained a reproducible threshold for different orientations, confirming that dislocations glide in the basal planes. This threshold is hysteretic because the force acting on dislocations depends on the pinning length L_i between impurities [17]. One now understands why Fig. 2 shows a ^3He pinning occurring at lower T with a large strain (10^{-7}) than with a low strain (10^{-9}). In contrast, the phonon damping is independent of the strain amplitude.

Fig. 5 shows additional measurements made on X4, a type 1 crystal that was cooled down under high strain (10^{-7}) at 3 kHz in order to expell all ^3He impurities into the liquid. Its coefficient c_{44} is reduced by 80% even at 20 mK. This value is stable in time (^3He stay trapped

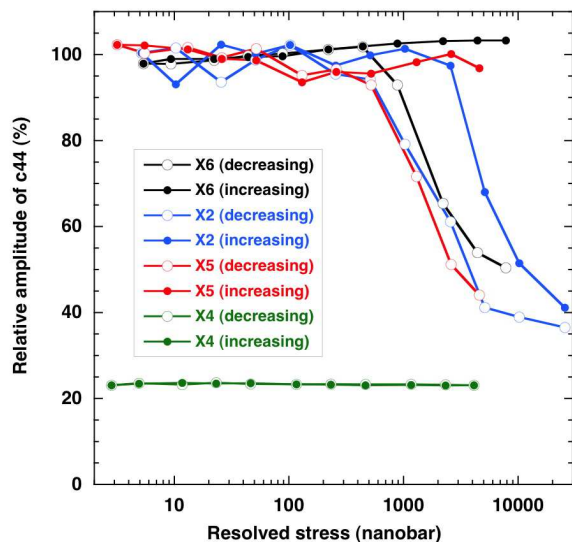


FIG. 5: The relative amplitude of c_{44} for 4 different crystals at 20 mK as a function of the stress projected on the basal plane ("resolved"). At a threshold stress around 1 microbar, dislocations break away from ^3He impurities [6, 13]. This threshold is larger when increasing the stress than when decreasing it. Being free of impurities, X4 shows a reduction of c_{44} by 80%, independent of stress.

in the liquid), and independent of the strain amplitude. After *assuming* that dislocations glide in the basal plane, Rojas *et al.* [9] found 86% reduction for a type 1 crystal of probably better quality (see Suppl. Mat.). Here we *demonstrate* that this assumption was correct, and that the plasticity is very large in particular directions. We have not yet prepared a crystal with zero dislocation as might be possible [18]. Dislocations arranged in a simple Frank network should lead to less than 5% reduction in c_{44} [19]. In our case, they may be aligned in sub-boundaries [22] where they cooperate to reduce c_{44} much more. Assuming a typical dislocation density [23] $\Lambda = 10^4 \text{ cm}^{-2}$, we could estimate the amplitude of their motion. With a 10 kHz strain $\varepsilon = 3 \cdot 10^{-8}$, we find that dislocations move a distance $d \sim \varepsilon/\Lambda b = 1 \text{ }\mu\text{m}$ at 1 cm/s ($b = 3 \text{ Angstrom}$ is the Burgers vector amplitude). This is 30 million Burgers vectors per second, a giant effect with no equivalent in classical crystals (see Suppl. Mat.) [19–21].

In summary, we have demonstrated that the plasticity of ^4He crystals is reversible and anisotropic, due to the free gliding of dislocations parallel to the basal planes. Classical plasticity is irreversible because dislocations jump from one pinning site to another and multiply, leading to "work hardening". In our case, applying large stresses at low T produces defects, which harden the crystals and are probably jogs because annealing at 1 K restores the high crystal quality (see Suppl. Mat.). For simplicity, we show measurements in this article, which are recorded on cooling after annealing. The giant plas-

ticity of ^4He crystals is mainly due to their absolute purity at very low temperature. An interesting question is whether dislocations move by tunnelling or by thermal activation over Peierls barriers. Tunnelling is suggested by the reversible motion at low T without dissipation or strain-dependence. However, quantum fluctuations probably reduce the kink energy E_k by enlarging their width. If $k_B T > E_k$, kinks are not relevant, as is the case for surface steps [24, 25] whose dynamics is also dissipation free in the low T limit. A calculation of E_k could indicate if the dislocation motion is quantum or classical thanks to a negligible kink energy.

This work was supported by grants from ERC (AdG 247258) and from NSERC Canada.

- [1] R. A. Vardanian, *Crystal Lattice Defects and Dislocation Dynamics* (Nova Science Pub. Inc., New York, 2000).
- [2] R.F. Tinder and J. Washburn, *Acta Met.* **12**, 129 (1964).
- [3] A. Berghezan, A. Fourdeux, and S. Amelinckx, *Acta Metall.* **9**, 464-490 (1961).
- [4] D. Hull and D.J. Bacon, *Introduction to Dislocations* (Butterworth-Heinemann Elsevier, Oxford, 2000).
- [5] L. Proville, D. Rodney, and M.C. Marinica, *Nature Mat.* **11**, 845-849 (2012).
- [6] J. Day and J. Beamish, *Nature* **450**, 853 (2007).
- [7] S. Sasaki, F. Caupin, and S. Balibar, *J. Low Temp. Phys.* **153**, 43 (2008).
- [8] C. Pantalei *et al.* *J. Low Temp. Phys.* **159**, 452 (2010).
- [9] X. Rojas, A. Haziot, V. Bapst, S. Balibar, and H.J. Maris, *Phys. Rev. Lett.* **105**, 145302 (2010).
- [10] S. Balibar, A.Y. Parshin, and H. Alles, *Rev. Mod. Phys.* **77**, 317-374 (2005).
- [11] O. Syshchenko, J. Day, and J. Beamish, *Phys. Rev. Lett.* **104**, 195301 (2010).
- [12] I. Iwasa, K. Araki, and H. Suzuki, *J. Phys. Soc. Japan* **46**, 1119 (1979).
- [13] J. Day and J.R. Beamish, *J. Low Temp. Phys.* **166**, 33 (2012).
- [14] R.H. Crepeau *et al.* *Phys. Rev. A* **3**, 1162 (1971).
- [15] D.S. Greywall, *Phys. Rev. B* **16**, 5127 (1977).
- [16] H.J. Maris and S. Balibar, *J. Low Temp. Phys.* **160**, 5 (2010).
- [17] I. Iwasa and H. Suzuki, *J. Phys. Soc. Jap.* **49**, 1722 (1980).
- [18] J.P. Ruutu *et al.* *Phys. Rev. Lett.* **76**, 4187 (1996).
- [19] J. Friedel, *Dislocations* (Pergamon, New York, 1964).
- [20] A. Hikata and C. Elbaum, *Phys. Rev. Lett.* **54**, 2418 (1985).
- [21] R. J. M. Farla *et al.*, *Science* **336**, 332 (2012).
- [22] I. Iwasa *et al.*, *J. Low Temp. Phys.* **100**, 147 (1995).
- [23] O. Syshchenko and J. Beamish, *J. Low Temp. Phys.* **150**, 276 (2008).
- [24] P. Nozières, *Eur. Phys. J. B* **24**, 383-386 (2001).
- [25] E. Rolley, E. Chevalier, C. Guthmann, and S. Balibar, *Phys. Rev. Lett.* **72**, 872 (1994); E. Rolley, C. Guthmann, E. Chevalier, and S. Balibar, *J. Low Temp. Phys.* **99**, 851 (1995).

The giant plasticity of a quantum crystal - Supplemental Material

Ariel Haziot¹, Xavier Rojas¹, Andrew D. Fefferman¹, John R. Beamish^{1,2}, and Sébastien Balibar¹

*1- Laboratoire de Physique Statistique de l'École Normale Supérieure,
associé au CNRS et aux Universités P.M. Curie and D. Diderot,
24 rue Lhomond, 75231 Paris Cedex 05, France.*

2 - Department of Physics, University of Alberta, Edmonton, Alberta Canada T6G 2G7

PACS numbers: 67.80.bd, 67.80.de, 67.80.dj

THE EXPERIMENTAL CELL AND THE TRANSDUCER CALIBRATION

Our experimental cell is a 5 cm³ hexagonal hole in a 15 mm thick copper plate, which is closed on its back and front faces by glass windows sealed with Indium rings (see Figure 1) and stainless steel clamps. It is filled with ⁴He through a thin Cu-Ni capillary (the "fill line" whose inner diameter is 0.4 mm). It stands at least 62 bar inner pressure. Inside this cell, we have glued two piezo-electric transducers [11] in order to shear crystals that are grown in the gap between them. The thickness of this gap was $d = 1.2$ mm in a first cell used for crystals from X1 to X6 and $d = 0.7$ mm in the second cell shown on Figure 1, where the transducers are glued on their whole surface area in order to avoid any possible

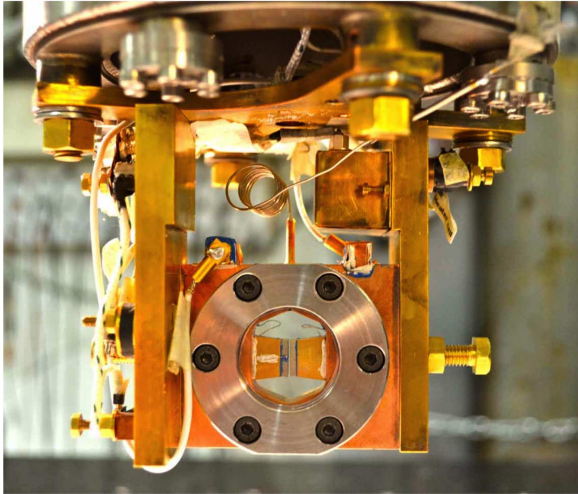


FIG. 1: The second cell used for this experiment is a 5 cm³ hole in a 15 mm thick Copper plate that is closed with two glass windows sealed with stainless steel clamps and Indium rings. The cell plate is attached to a dilution refrigerator which allows measurements down to 15 mK. ⁴He crystals are grown inside the 0.7 mm gap between two piezo-electric transducers by injecting liquid through a 0.4 mm capillary on the top (see Figure 2). The two transducers allow applying a vertical shear and measuring the resulting stress across the thin crystal in the gap. A first cell was used for this experiment, where the gap was 1.2 mm thick. The optical access allows determining the crystal orientation (see Figure 3).

bending near their edges. Figure 2 shows the "loading curve", that is the stress measured as crystallization proceeds from the bottom to the top of the transducers. Note that this curve shows no particular singularity at half loading when the liquid-solid interface passes over the two soldering points of grounding leads that are visible on Figure 3. One of these soldering points is on the front and the other on the back so that there is no significant variation in the gap thickness there. Figure 3a shows the shape of a seed during fast growth, which is used to determine the crystal orientation before the crystal is regrown more slowly over the entire cell including the gap between the two transducers (Figure 3b). An ac-voltage (1 mV to 1V at a frequency in the range 1 to 20 000 Hz) is applied to one transducer, which produces a vertical displacement u , consequently a strain $\varepsilon = u/d$ and finally a stress $\sigma = \mu\varepsilon$ on the other transducer (μ is the shear modulus of the He crystal). The displacement u is very small - of order 1 Angstrom per Volt - and it needs to be accurately calibrated in order to obtain an absolute value for μ . The stress generates charges, which are collected as a current whose amplitude and phase are measured with a lock-in amplifier. We also use current pre-amplifiers (femto-lca-20k-200m and femto-lca-200-10g) as was done by Day and Beamish who introduced this method in their original work [2]. We improved their method by calibrating the transducers' response in the following way. We first measured the cross talk between transducers. Although the transducer sides facing each other are grounded, there is a small cross talk between them, which mainly comes from capacitive coupling and needs to be accurately known as a function of frequency. It is independent of pressure and temperature in our working conditions so that we measured it with the cell full of liquid. As explained in the main text, we then used a particular crystal (X3), which was oriented with a [0001] axis tilted by an angle very close to 45° from vertical. For this crystal, the response to a vertical shear depends mainly on the three elastic coefficients c_{11} , c_{13} and c_{33} , with a negligible contribution from c_{44} and c_{66} . The coefficients c_{44} and c_{66} contribute to the shear modulus in all directions except for a shear at 45° from the [0001] axis. We then verified that the measured shear modulus was independent of temperature in our geometry for this particular crys-

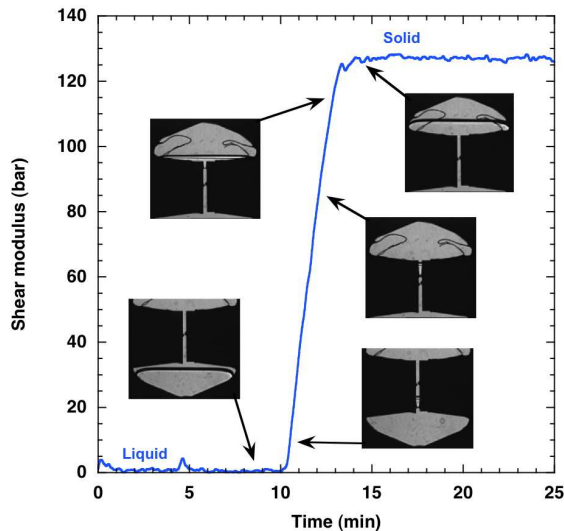


FIG. 2: The loading curve is the shear stress measured in the cell as a function of time during the growth of the crystal in the gap, which takes about 3 minutes in this case. Near the mid height of the transducers, one sees two point contacts for the grounding of the transducer surfaces that face each other. One of these contacts is on the front and the other on the back side of the transducer, so that there is no significant variation in the gap thickness there. Thanks to this design, the loading curve shows a linear variation with height with no singularity at half loading.

tal (see Fig. 3 in the main text). Finally, we used the known values [7, 8] of c_{11} , c_{13} and c_{33} to obtain the piezoelectric coefficient we needed. In the first cell it was $d_{15} = 0.88$ Angstrom/Volt independently of T up to 1 K and 0.95 in the second cell, about 5 times less than at room temperature. The shear modulus is $\mu = Id/(\omega d_{15}^2 A \sigma)$, where V is the voltage applied to the first transducer, A is the transducers' area (1.2 cm² in the first cell and 1 cm² in the second one), I is the current generated by the stress on the second transducer. In order to know I , a careful calibration of the gain of our amplifiers needed to be done as a function of frequency. In the end we obtained the absolute amplitude of the real and imaginary part of the response, that is the shear modulus μ and the dissipation $1/Q = \tan(\phi)$ where ϕ is the phase delay of the response. For each crystal orientation, we calculated μ as a function of the 5 elastic coefficients (see below), so that we could extract the variation of c_{44} .

SAMPLE PREPARATION

The quality and the purity of samples are very important in this experiment. The crystal quality depends on growth conditions as previously explained by Sasaki *et al.* [3] and by Pantalei *et al.* [4]. The best crystals, called "type 1", are grown relatively slowly (up to 50 $\mu\text{m/s}$ in

this experiment, 0.3 $\mu\text{m/s}$ in the experiment by Rojas *et al.* [5]) at low T , usually around 20 mK, by pressurizing superfluid ⁴He up to the liquid-solid equilibrium pressure $P_{eq} = 25.3$ bar. After nucleation on a random site, a crystal seed grows, falls down to the bottom part of the cell and the growth proceeds at constant T and P thanks to the mass injection into the cell through the fill line where helium remains liquid. This fill line is thermally anchored along its path to the cell, so that growth does not warm up the cell even at temperatures less than 20 mK in this experiment. At the equilibrium or during slow growth, the crystal occupies the lower part of the cell with a horizontal surface and some capillary effects where it touches the walls, as would a non-wetting liquid in a little glass bottle. This is because the growth dynamics proceeds with negligible dissipation and because the temperature is highly homogeneous so that there are no temperature gradients, only a gravity field [1]. In order to fill the cell with solid as much as possible, one has to place the orifice of the fill line at the highest point in the cell. For this purpose, our cells are tilted. One also has to avoid corners or slits where liquid would be trapped because of capillary effects. Finally, it is also important to avoid the presence of dust particles on walls because they are efficient pinning sites for the liquid-solid interface moving up. If one stays at P_{eq} at the end of the growth, there necessarily remains some liquid in corners or slits, in our case at the junction between the glass windows and the cell body. As a consequence, the ³He impurities may be trapped in this liquid if growth takes place at low T , because their solubility in the liquid is much higher than in the solid [4]. According to our experience, it is also possible to expel all ³He impurities in this adjacent liquid by applying a large ac-stress on the crystal at low T , because the resulting force shakes the dislocation and detaches them from the ³He atoms that are known to travel ballistically through the crystal lattice so that they reach liquid regions in a short time and stay trapped there.

We use a different growth procedure for "type 2" crystals. We grow them again at constant T and P from the superfluid liquid, but at 1.4 K. When the cell is as full of solid as possible, we block the fill line by increasing the pressure outside and we cool down to 1 K at constant volume. Due to the decrease of P_{eq} from 26.1 bar at 1.4 K to 25.3 bar at 1 K, the rest of the liquid in the cell crystallizes but the quality of the final crystal, which occupies the whole cell now, is expected to be damaged by stresses. The advantage of this method is that it produces a crystal in which the ³He concentration is known, equal to the initial concentration in the gas cylinder, and stays at this value during temperature cycles afterwards. Since it is easy to melt or grow crystals by manipulating valves outside the refrigerator, we could melt any "type 1" crystal to a small seed and regrow it as a "type 2" crystal or vice versa.

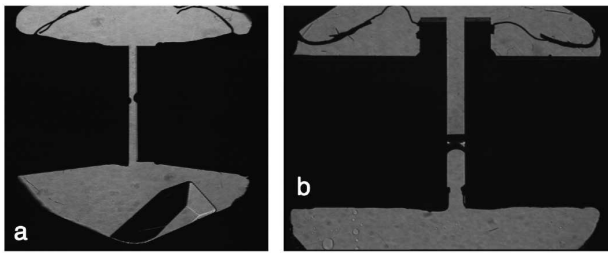


FIG. 3: Two photographs showing the growth shape of a seed crystal on the left (a), and the growth inside the gap on the right (b). The total width of the cell is 20 mm. The growth of the seed is fast enough (1 mm/s) to make facets visible on the left photograph (a) and to allow the determination of the crystal orientation (here crystal X3 with its c axis tilted at 45° from the vertical). The growth inside the gap is shown on the right photograph (b). Here it is our first cell where the gap is slightly larger, 1.2 mm instead of 0.7. The growth inside the gap is slower ($50 \mu\text{m/s}$). In this first cell, the two transducers were not glued on their entire surface and the electrical contacts were made on the bottom edge of the transducers. Between the two transducers, one can see a straight horizontal line, which is the solid-liquid interface outside the gap, and a convex one below, which shows the capillary depression of the meniscus inside the gap. This depression is a consequence of a 45° contact angle with the transducer walls (for more details on this partial wetting, see [6]).

”Type 3” crystals are polycrystals grown at constant volume from the normal liquid above the superfluid transition. This is known as the ”blocked capillary” (BC) method because, when cooling starts, a solid plug forms in the fill line near the ”1K pot” of the refrigerator after what the growth proceeds at constant volume and constant mass (but at varying P and T of course). In this experiment, we started cooling down the cell around 3 K with 60 bars everywhere. In the cell, the crystallization started at 2.4 K and finished at 1.7 K with a final pressure $P = 30$ bar (see ”path A” in the phase diagram of ref. [3]). We chose these values to avoid crossing the reappearance of liquid near the hcp-bcc transition of the solid (see [3]). Indeed, recrystallization from the superfluid usually ends up with a few large single crystals while our goal was to obtain isotropic polycrystals with small grains and a strong disorder. The polycrystalline nature of the sample is probably a consequence of multiple nucleations of seeds in a cell that is far from homogeneous in temperature in the absence of superfluid. We found that the crystals grown at the lowest temperature have the largest softening, that is the largest reduction of c_{44} in the soft state. This is probably because their dislocation density Λ is smaller, with a larger free length L between pinning sites (a larger ”pinning length”). The precise measurement of Λ and L is in progress in our laboratory.

In this experiment, we reached 80% reduction of c_{44} with the ”type 1” crystal X4. In a previous experiment,

Rojas *et al.* [5] had found an 86% reduction of c_{44} , after assuming that no other elastic constant varied, for another ”type 1” crystal which was probably of even better quality for two reasons. First, the growth rate used by Rojas *et al.* was significantly lower ($0.3 \mu\text{m/s}$) than in this experiment ($50 \mu\text{m/s}$). Secondly, Rojas’ cell had a much more open geometry with no corners and a larger horizontal cross section area, which allowed much more continuous growth without sharp jumps each time the liquid-solid interface detaches from some pinning site.

In their experiment, Ruutu *et al.* [10] obtained small crystals with no screw dislocations according to their measurements of growth rates. Their crystals were grown slowly at 20 mK, but the dislocation density probably depends on the growth speed just after nucleation, which is difficult to monitor. We have not yet succeeded in preparing crystals without any dislocation but it is obviously an exciting challenge because we expect the disappearance of plasticity in that case.

ORIENTATION DEPENDENCE

A little geometry has been necessary for the data analysis. The elastic tensor of an hcp crystal involves 5 independent coefficients c_{ij} with values of i, j from 1 to 6 and writes:

$$\begin{pmatrix} c_{11} & c_{12} & c_{13} & 0 & 0 & 0 \\ c_{12} & c_{11} & c_{13} & 0 & 0 & 0 \\ c_{13} & c_{13} & c_{33} & 0 & 0 & 0 \\ 0 & 0 & 0 & c_{44} & 0 & 0 \\ 0 & 0 & 0 & 0 & c_{44} & 0 \\ 0 & 0 & 0 & 0 & 0 & c_{66} \end{pmatrix}$$

The meaning of these indices from 1 to 6 is respectively xx , yy , zz , yz , xz and xy with the z -axis parallel to [0001], the six-fold symmetry axis - also called ” c ” - of the hexagonal structure. The coefficient $c_{66} = (c_{11} - c_{12})/2$. The orientation of the x -axis in the plane perpendicular to the c axis is arbitrary since we assume that the dislocations are distributed such that the transverse isotropy of the hcp crystal is preserved. In our experiment, the axis c is tilted with respect to the vertical direction z' of the shear. The crystal orientation is given by the angles θ and ϕ as defined on Figure 4 where the growth shape is compared with a hexagonal prism. Coordinate transformations can be applied to quantities expressed in abbreviated notation using the Bond matrices [14]. Rotations of the coordinate system about its y -axis are applied with:

$$M_y(\eta) = \begin{pmatrix} \cos^2\eta & 0 & \sin^2\eta & 0 & -\sin 2\eta & 0 \\ 0 & 1 & 0 & 0 & 0 & 0 \\ \sin^2\eta & 0 & \cos^2\eta & 0 & \sin 2\eta & 0 \\ 0 & 0 & 0 & \cos\eta & 0 & \sin\eta \\ \frac{1}{2}\sin 2\eta & 0 & -\frac{1}{2}\sin 2\eta & 0 & \cos 2\eta & 0 \\ 0 & 0 & 0 & -\sin\eta & 0 & \cos\eta \end{pmatrix}$$

and rotations about its z-axis are applied with:

$$M_z(\xi) = \begin{pmatrix} \cos^2\xi & \sin^2\xi & 0 & 0 & 0 & \sin 2\xi \\ \sin^2\xi & \cos^2\xi & 0 & 0 & 0 & -\sin 2\xi \\ 0 & 0 & 1 & 0 & 0 & 0 \\ 0 & 0 & 0 & \cos\xi & -\sin\xi & 0 \\ 0 & 0 & 0 & \sin\xi & \cos\xi & 0 \\ -\frac{1}{2}\sin 2\xi & \frac{1}{2}\sin 2\xi & 0 & 0 & 0 & \cos 2\xi \end{pmatrix}$$

The elastic tensor in the transducer coordinate system $x'y'z'$ (Figure 4) is given by:

$$C' = M_z(-\phi)M_y(-\theta)CM_y^T(-\theta)M_z^T(-\phi)$$

where X^T is the transpose of matrix X .

The shear modulus that relates the shear strain we apply to the component of the shear stress that we measure is given by:

$$\mu = c'_{44} = \frac{1}{4}(c_{11} - 2c_{13} + c_{33})\sin^2 2\theta \sin^2 \phi + c_{44}(\cos^2 \theta \cos^2 \phi + \cos^2 2\theta \sin^2 \phi) + c_{66} \cos^2 \phi \sin^2 \theta$$

We used the above equation to calculate the shear modulus μ as a function of the coefficients c_{ij} for all our crystals. For example we obtained:

$$\mu = 0.0001(c_{11} - 2c_{13} + c_{33}) + 0.933c_{44} + 0.067c_{66} \text{ for X2} \\ (\theta = 89.5^\circ \text{ and } \phi = 85^\circ)$$

$$\mu = 0.25(c_{11} - 2c_{13} + c_{33}) + 0.004c_{44} + 0.004c_{66} \text{ for X3} \\ (\theta = 45^\circ \text{ and } \phi = 85^\circ)$$

$$\mu = 0.0001(c_{11} - 2c_{13} + c_{33}) + 0.25c_{44} + 0.56c_{66} \text{ for X5} \\ (\theta = 60^\circ \text{ and } \phi = 30^\circ)$$

$$\mu = 0.008(c_{11} - 2c_{13} + c_{33}) + 0.97c_{44} \text{ for X21} \\ (\theta = 5^\circ \text{ and } \phi = 90^\circ)$$

The values of all c_{ij} have been obtained from ultrasound velocity measurements at 10 MHz by Crepeau *et al.* at 1.32K [7] and by Greywall at 1.2K [8] $c_{11} = 405$ bar, $c_{12} = 213$ bar, $c_{13} = 105$ bar, $c_{33} = 554$ bar, $c_{44} = 124$ bar, and $c_{66} = 96$ bar. At such high temperatures, the damping of dislocation motion by thermal phonons being proportional to the frequency and to T^3 , [12] dislocations cannot move at 10 MHz. As a consequence, their values correspond to the true elasticity of the lattice, without any contribution from plasticity. We have verified that, at low temperature in the presence of ^3He impurities, the shear modulus of our ^4He crystals is the

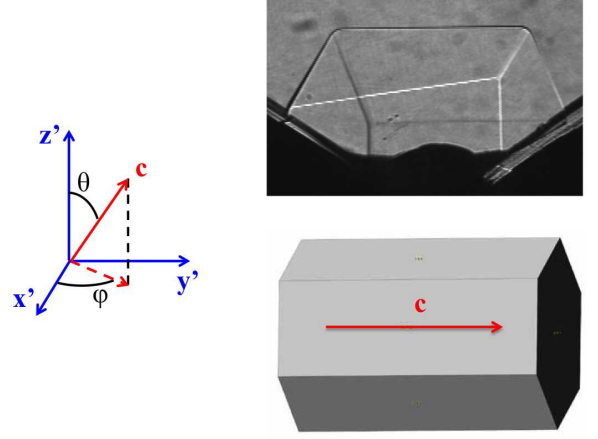


FIG. 4: The crystal orientation. The orientation of the [0001] axis "c" is defined by two angles θ and ϕ . The axis z' is vertical, parallel to the transducer plane surfaces. The axis x' is perpendicular to the windows, and the axis y' is perpendicular to the transducer surfaces. The values of θ and ϕ are obtained by matching the growth shape with a hexagonal prism. In this particular case (crystal X2), the c axis is very close to horizontal. On the photograph, one sees that the crystal touches the front window so that two white lines correspond to intersections of the crystal with this front window. Only the free edges of the crystal are used to determine the orientation.

same as measured by Crepeau *et al.* [7] and by Greywall [8]. The only correction to be made for polycrystals grown at high pressure is the pressure dependence analysed by H.J. Maris [9].

The resolved stress σ_r is the quantity which determines the force acting on dislocations. We determined it as follows. The strain in the transducer coordinate system (Figure 4) is given by:

$$E' = (0 \ 0 \ 0 \ \varepsilon \ 0 \ 0)^T$$

In the crystal frame this becomes:

$$E = M_y(\theta)M_z(\phi)E'$$

The stress in the crystal frame is then :

$$\Sigma = CE$$

The magnitude of the resultant of the shear stresses acting in the basal plane $(\Sigma_4^2 + \Sigma_5^2)^{1/2}$ is independent of rotations of the crystal about its c -axis. If we assume that the three $\langle 11\bar{2}0 \rangle$ Burgers vectors are uniformly populated then we can choose the convenient orientation with one set of Burgers vectors along the stress resultant and the other two at 60° to it. Then the average resolved stress will be:

$$\sigma_r = \frac{c_{44}\varepsilon \sqrt{\cos^2 \theta \cos^2 \phi + \cos^2 2\theta \sin^2 \phi}}{\sqrt{3}}$$

TEMPERATURE CYCLES AND ANNEALING OF SAMPLES

Most of the data that are analysed in this article have been obtained by cooling samples slowly (12 hours) from 1 K down to 15 mK. The first reason for proceeding this way is that we confirmed that some disorder induced by mechanical perturbations at low T is annealed when warming above 0.5 K, as was previously noticed by Day *et al.* [12]. Each temperature cycle took 6 hours for warming up to 1 K and 12 hours for cooling down to 15 mK, that is about one day. We used the same procedure for all crystals in order to include a recording during the night when perturbations from the environment were as small as possible (remember that we measure stresses down to 1 nanobar; He crystals are extremely sensitive to vibrations). We then transferred liquid Nitrogen every morning when the crystal was cold. Every three days, a liquid helium transfer was also necessary to keep the refrigerator working. All these transfers produce mechanical vibrations that shake dislocations. After any large mechanical perturbation at low temperature, we observe some hardening of crystals, which we believe is due to creation of jogs on the dislocations. After annealing up to 1 K we found reproducible results as if jogs had been eliminated thanks to the diffusion of thermally activated vacancies.

COMPARISON WITH A CLASSICAL CRYSTAL

In order to compare the plasticity in helium crystals and in classical crystals, let us consider the historical measurements by Tinder and Washburn[15] on Copper. Qualitatively, the plasticity is the same phenomenon: it is due to the motion of dislocations and it is sensitive to the concentration of impurities. But quantitatively, there are striking differences. Tinder and Washburn found a threshold stress of about $2 \text{ g/mm}^2 = 2 \cdot 10^4 \text{ Pa}$ beyond which a plastic strain appears in addition to the usual elastic response. This threshold is somewhat smaller than in other classical crystals, probably because of the careful growth and manipulation of these very pure samples. Still, it is larger by five orders of magnitude than in our case. In Copper, the applied stress is $0.4 \cdot 10^{-6}$ times the shear modulus $\mu_{Cu} = 50 \text{ GPa}$. For helium crystals, we find a linear response (no threshold) down to 1 nanobar = 10^{-4} Pa , which is 10^{-11} times the elastic shear modu-

lus $\mu_{He} = 12 \text{ MPa}$. Furthermore, Tinder and Washburn find a plastic strain that is 40 times *smaller* than the elastic strain so that the effective shear modulus is not significantly changed. In Helium, the plastic strain due to the dislocation motion is 4 times *larger* than the elastic strain, leading to an effective shear modulus that is reduced by 80%. In other words, the plastic response is 2 orders of magnitude larger for stresses 5 orders of magnitude smaller than in Copper. In Copper, the plastic response is highly non-linear and the response time of order minutes at room temperature (300 K). In Helium at 0.1 K, the plasticity is linear so that it results in an effective reduction of the shear modulus, which we have found independent of frequency up to 16 kHz. We have been able to study oriented single crystals and we have found evidence that the gliding plane of dislocations is the basal plane, so that the plasticity is anisotropic. Tinder and Washburn studied polycrystalline samples where they could not measure any orientation dependence of the plasticity.

This work was supported by grants from ERC (AdG 247258-SUPERSOLID) and from NSERC Canada.

-
- [1] A. Berghezan, A. Fourdeux, and S. Amelinckx, *Acta Metall.* **9**, 464-490 (1961).
 - [2] J. Day and J. Beamish, *Nature* **450**, 853 (2007).
 - [3] S. Sasaki, F. Caupin, and S. Balibar, *J. Low Temp. Phys.* **153**, 43 (2008).
 - [4] C. Pantalei et al. *J. Low Temp. Phys.* **159**, 452 (2010).
 - [5] X. Rojas, A. Haziot, V. Bapst, S. Balibar, and H.J. Maris, *Phys. Rev. Lett.* **105**, 145302 (2010).
 - [6] S. Balibar, A.Y. Parshin, and H. Alles, *Rev. Mod. Phys.* **77**, 317-374 (2005).
 - [7] R.H. Crepeau et al. *Phys. Rev. A* **3**, 1162 (1971).
 - [8] D.S. Greywall, *Phys. Rev. B* **16**, 5127 (1977).
 - [9] H.J. Maris and S. Balibar, *J. Low Temp. Phys.* **160**, 5 (2010).
 - [10] J.P. Ruutu et al. *Phys. Rev. Lett.* **76**, 4187 (1996).
 - [11] PZT ceramics from Boston Piezo-Optics Inc., USA.
 - [12] J. Day, O. Syshchenko, and J. Beamish, *Phys. Rev. B* **79**, 214524 (2009).
 - [13] A. V. Granato and K. Lcke, *J. Appl. Phys.* **27**, 583 (1956).
 - [14] B. A. Auld, *Acoustic Fields and Waves in Solids*, Vol. 1, (Krieger, Malabar, 1990).
 - [15] R.F. Tinder and J. Washburn, *Acta Met.* **12**, 129 (1964).